Laser Magnetic Resonance of the NO Molecule Using 78-, 79-, and 119-μm H_2O Laser Lines*

Masataka Mizushima
Department of Physics and Astrophysics, University of Colorado, Boulder, Colorado 80302

and

K. M. Evenson and J. S. Wells
National Bureau of Standards, Boulder, Colorado 80302

(Received 24 November 1971)

The magnetic resonance of the NO molecule is observed using the 78-, 79-, and 119-μm lines of the H_2O laser as the radiation source. The resonances in three cases are due to the $(^2\Pi_{1/2} J=12.5) \rightarrow (^2\Pi_{3/2} J=12.5)$, $(^2\Pi_{1/2} J=11.5) \rightarrow (^2\Pi_{3/2} J=11.5)$, and $(^2\Pi_{1/2} J=12.5) \rightarrow (^2\Pi_{3/2} J=11.5)$ transitions, respectively. Most of them are magnetic dipole transitions, but a few electric dipole transitions are also observed. It is found that the calculated g factors $g_{c2}(11.5)=g_{d2}(11.5)=-0.0064$, $g_{c1}(11.5)=g_{d1}(11.5)=0.0272$, $g_{c2}(12.5)=g_{d2}(12.5)=-0.0092$, $g_{c1}(12.5)=g_{d1}(12.5)=0.0270$, and the calculated Λ-doublet separations $f_{c2}(11.5)-f_{d2}(12.5)=243$ MHz, $f_{c1}(11.5)-f_{d1}(11.5)=4323$ MHz, are consistent with our experimental results. The hyperfine structure and the second-order effects are also in agreement with theoretical values. The average separation between the $^2\Pi_{3/2}$ and $^2\Pi_{1/2}$ states for a given J, which we call X_J, is found to be 126.4469 ± 0.0005 and 127.5786 ± 0.0005 cm^{-1} for $J=11.5$ and 12.5, respectively. The conventional spin-orbit coupling constant is found to be 123.1580 ± 0.0010 cm^{-1} when $J=12.5$ or 11.5. [The conventional spin-orbit coupling constant A_c, commonly referred to as A, is given by $A-\delta(J+\frac{1}{2})^2+\frac{1}{4}\gamma$ in our notation.] The coupling constant μ_S for the $\vec{S}\cdot\vec{N}$ term is found to be -0.006 ± 0.002 cm^{-1}.

I. INTRODUCTION

The $^2\Pi$ ground electronic state of nitric oxide is split into $^2\Pi_{1/2}$ and $^2\Pi_{3/2}$ states by the spin-orbit coupling with the $^2\Pi_{1/2}$ state having the lower energy. The end-over-end rotation mixes these two electronic states, but since the rotation constant B is very small compared to the spin-orbit coupling constant A, the mixing effect is much smaller than in the case of the OH free radical, which also is the $^2\Pi$ state.[1] Since the electronic angular momentum in the $^2\Pi_{1/2}$ and $^2\Pi_{3/2}$ states can be either along or opposite to the direction of the molecular axis, each state is doubly degenerate. The degeneracy is slightly removed due to the end-over-end rotation, and the Λ doublet is formed.[2] Thus, there are four energy levels for a given total angular momentum quantum number J.

Some energy levels in the vibrational ground state of $N^{14}O^{16}$ are illustrated in Fig. 1 (Ref. 3). Hall and Dowling[4] observed infrared absorption due to $\Delta J=1$ transitions among each series of $^2\Pi_{1/2}$ and $^2\Pi_{3/2}$ for J of 4.5 up to 26.5. In microwave spectroscopy similar transitions of $J=0.5 \rightarrow 1.5$ and $1.5 \rightarrow 2.5$ are observed by Burrus and Gordy,[5] Gallagher and Johnson,[6] and Favero, Mirri, and Gordy.[7] Recently, Dymanus[8] observed several transitions among the Λ doublets by means of the molecular-beam-resonance technique. Vibrational transitions have been observed by James and Thibault[9] and Keck and Hause,[10] and they reported dependable values of the spin-orbit coupling constant A.

In this paper we report the first observations[3] of transitions from $^2\Pi_{1/2}$ to $^2\Pi_{3/2}$ states detected by a laser-magnetic-resonance technique. The energy levels were Zeeman shifted into coincidence with the 78-, 79-, and 119-μm lines of the H_2O laser. The technique is similar to the previous one we used in investigating laser magnetic resonances of the O_2,[11,12] OH,[13] and CH[14] molecules.

The Zeeman effect of the $J=0.5 \rightarrow 1.5$ transition has been studied by Mizushima, Cox, and Gordy,[15] and some microwave magnetic resonances have been observed by Beringer and Castle.[16]

II. GENERAL THEORY

The four energy levels with a given J quantum number have been discussed by Van Vleck,[2] and Dousmanis, Sanders, and Townes.[17] MM[1] and Veseth[18] took into account the centrifugal distortion effects; to a good approximation MM's result[1] can be written as

$$f_{c2}(J)=\xi_J+\eta_J+\tfrac{1}{2}X_J+(Y_J/4X_J), \tag{1a}$$

$$f_{d2}(J)=\xi_J-\eta_J+\tfrac{1}{2}X_J-(Y_J/4X_J), \tag{1b}$$

$$f_{c1}(J)=\xi_J+\eta_J-\tfrac{1}{2}X_J-(Y_J/4X_J), \tag{1c}$$

$$f_{d1}(J)=\xi_J-\eta_J-\tfrac{1}{2}X_J+(Y_J/4X_J), \tag{1d}$$

where

$$\xi_J=(B-\beta-D)(J+\tfrac{1}{2})^2-D(J+\tfrac{1}{2})^4+\cdots, \tag{2a}$$

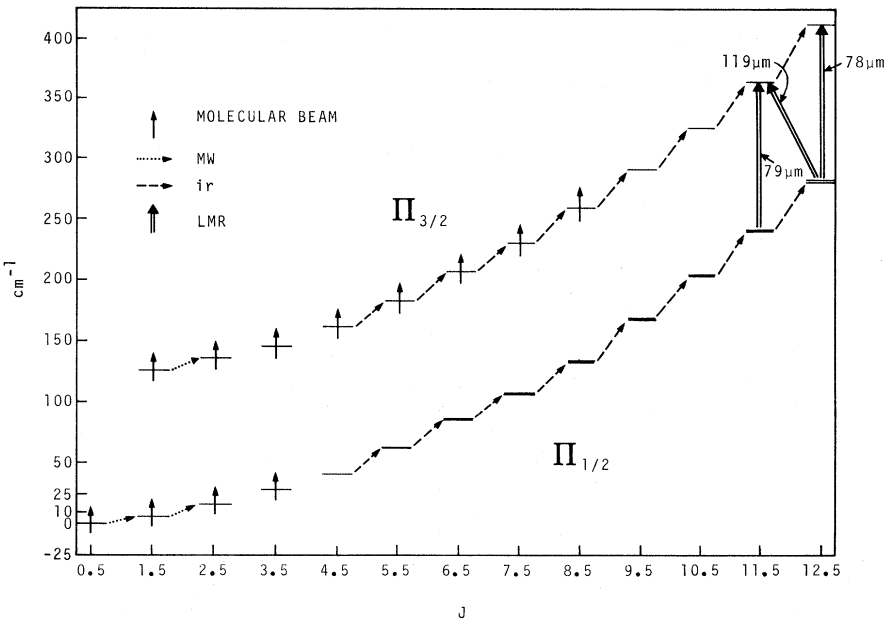

FIG. 1. Rotational energy levels of the NO molecule in the $^2\Pi\, v=0$ state. The Λ doublets are too small to be shown in this scale except in some high J states. hfs are too small to be shown. Some pure rotational transitions are observed in microwave and infrared spectroscopy, and transitions within each Λ doublet are observed in molecular beam spectroscopy. Observed (Ref. 3) transitions are indicated by arrows and transitions reported in the present paper are indicated by double arrows.

$$\eta_J = \tfrac{1}{2}(\alpha+\lambda)(J+\tfrac{1}{2}) - (\epsilon+\kappa)(J+\tfrac{1}{2})^3 + \cdots , \tag{2b}$$

$$X_J = \{\overline{A}_J^2 + 4\overline{B}_J^2[(J+\tfrac{1}{2})^2 - 1]\}^{1/2} , \tag{2c}$$

$$Y_J = -2\overline{A}_J(\alpha+\lambda)(J+\tfrac{1}{2}) + 8\overline{B}_J\beta(J+\tfrac{1}{2})[(J+\tfrac{1}{2})^2 - 1] . \tag{2d}$$

In (2c) and (2d) we note that

$$\overline{A}_J = A - 2B + \beta + \tfrac{1}{4}\gamma - 2(\delta - 2D)(J+\tfrac{1}{2})^2 + \cdots , \tag{3a}$$

$$\overline{B}_J = B - \tfrac{1}{2}\mu_S - \tfrac{1}{2}\alpha - 2D(J+\tfrac{1}{2})^2 + \cdots . \tag{3b}$$

All molecular parameters are defined in MM.[1] The most important ones, A and B, are the spin-orbit coupling constant and the rotational constant, respectively. The Λ-doublet splittings are given by α and β, which correspond to p and q of Mulliken and Christy.[19] Other parameters are expected to be negligible for a rough estimation of energy levels.

Formulas (1a) through (1d) give the energies of the four levels with a given J. The energy levels ($c2$) and ($d2$) are close to each other and higher than the other pair ($c1$) and ($d1$) by X_J. In the case of NO the ($c2$) and ($d2$) states reduce to $^2\Pi_{3/2}$ states, while the ($c1$) and ($d1$) states reduce to $^2\Pi_{1/2}$ states, if B is zero. The situation is opposite in the case of the OH free radical. Since $B \ll A$ in the present case we can call the ($c2$) and ($d2$) states as $^2\Pi_{3/2}$ and the ($c1$) and ($d1$) states as $^2\Pi_{1/2}$ to a good approximation.

James and Thibault[9] and Hall and Dowling[4] obtained a value of 123.160 cm^{-1}, for the conventional spin-orbit coupling constant A_c while Keck and Hause[10] proposed another value 123.21 cm^{-1}. Gallagher and Johnson,[6] Hall and Dowling,[4] and Keck and Hause[10] reported the values of B and D as 1.695 79 and 5.5×10^{-6} cm^{-1}, respectively. When the larger value of A_c is taken and all other parameters in (2c), except for B and D, are neglected, we obtain

$$X_J = \begin{cases} 126.49 \text{ cm}^{-1} & \text{for } J = 11.5 \\ 127.61 \text{ cm}^{-1} & \text{for } J = 12.5 . \end{cases} \tag{4}$$

Since the 79- and 78-μm lines of the H_2O laser have the wave numbers[19,20] of 126.4367 and 127.4808 cm^{-1}, respectively, we see that the laser resonance we observed by means of these lines are due to the $^2\Pi_{1/2} \rightarrow {}^2\Pi_{3/2}$ transitions at $J = 11.5$ and 12.5, respectively. Combining these theoretical values of X_J with the observed[4] wave number 42.93 cm^{-1} for the transition $J = 11.5 \rightarrow 12.5$ in the $^2\Pi_{3/2}$ state, we see that the transition ($^2\Pi_{1/2}\, J = 12.5$) $\rightarrow$ ($^2\Pi_{3/2} J = 11.5$) must appear at 84.62 cm^{-1}. Since the wave number of the 119-μm line of the H_2O laser is[21,22] 84.323 42 cm^{-1} the resonance we observed using this line must be due to the above transition. These assignments are shown in Fig. 2.

For the Λ-doublet constants α and β Gallagher and Johnson[6] proposed the values 176.15 and 1.15 MHz, respectively. From the recent data by Dymanus,[8] however, we see that[23] 178.05 and 1.421 MHz are more plausible values for these molecular parameters. If we neglect δ, λ, ϵ, and κ in (2b) and (2d) we obtain the theoretical Λ-doublet splittings as

$$f_{c2}(11.5) - f_{d2}(11.5) = 243 \text{ MHz}, \tag{5a}$$

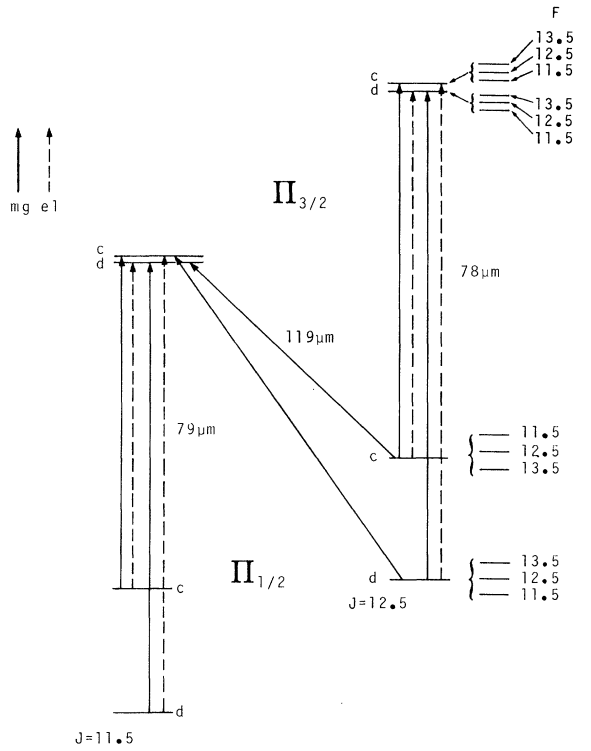

FIG. 2. Schematic energy level diagram and the transitions observed by means of the laser magnetic resonance method. The Λ doublets are exaggerated by a factor of 10, and the hfs are exaggerated by a factor of about 100.

$$f_{c1}(11.5) - f_{d1}(11.5) = 4030 \text{ MHz}, \tag{5b}$$

$$f_{c2}(12.5) - f_{d2}(12.5) = 306 \text{ MHZ}, \tag{5c}$$

$$f_{c1}(12.5) - f_{d1}(12.5) = 4323 \text{ MHz}. \tag{5d}$$

The hyperfine structure (hfs) of $N^{14}O$ is due to the nitrogen nucleus which has spin one. The magnetic hfs in each state can be written as

$$\mathcal{A}_J \frac{F(F+1) - J(J+1) - I(I+1)}{2J(J+1)} , \tag{6}$$

where

$$\mathcal{A}_{c2} = \mathcal{A}_\xi + \mathcal{A}_\eta + \mathcal{A}_X + \mathcal{A}_Y , \tag{7a}$$

$$\mathcal{A}_{d2} = \mathcal{A}_\xi - \mathcal{A}_\eta + \mathcal{A}_X - \mathcal{A}_Y , \tag{7b}$$

$$\mathcal{A}_{c1} = \mathcal{A}_\xi + \mathcal{A}_\eta - \mathcal{A}_X - \mathcal{A}_Y , \tag{7c}$$

$$\mathcal{A}_{d1} = \mathcal{A}_\xi - \mathcal{A}_\eta - \mathcal{A}_X + \mathcal{A}_Y , \tag{7d}$$

neglecting the second-order effect. In these formulas

$$\mathcal{A}_\xi = a + \tfrac{1}{4}(b+c) - \tfrac{1}{4}(b'+c')(J+\tfrac{1}{2})^2 , \tag{8a}$$

$$\mathcal{A}_\eta = \tfrac{1}{4} d (J+\tfrac{1}{2}), \tag{8b}$$

$$\mathcal{A}_X = (1/2X_J)\{A_J(a+b+c) - A_J(b'+c')(J+\tfrac{1}{2})^2 - 2B_J b[(J+\tfrac{1}{2})^2 - 1]\} , \tag{8c}$$

$$\mathcal{A}_Y = [(J+\tfrac{1}{2})/4X_J] A_J d , \tag{8d}$$

where a, b, c, and d are the coupling constants defined by Frosch and Foley[24] and Dousmanis.[25] The centrifugal distortion effect on b and c produces b' and c' terms, respectively. Some values for a, b, c, and d coupling constants were proposed by Dousmanis,[25] Mizushima,[26] and Gallagher and Johnson,[6] but no combination of these a, b, c, and d can explain the recent data by Dymanus.[8] It is found that $b'+c'$ term, which has been neglected so far, is important[2] in the case of this molecule, and when this term is taken into account, the values of other constants are changed drastically. The values which fit the new[8] and old[5–7] data are

$$a = 7.6, \quad b = 86.2, \quad c = -253.5, \quad d = 112.6, \quad b'+c' = -2.252 \text{ MHz}. \tag{9}$$

When these values are used in formulas (7) and (8), we obtain

$$\mathcal{A}_{c2} = -36.1, \quad \mathcal{A}_{d2} = -16.1, \quad \mathcal{A}_{c1} = 890, \quad \mathcal{A}_{d1} = -555.1 \text{ MHz} \quad \text{for } J = 11.5; \tag{10a}$$

$$\mathcal{A}_{c2} = -23.6, \quad \mathcal{A}_{d2} = 1.8, \quad \mathcal{A}_{c1} = 890.0, \quad \mathcal{A}_{d1} = -599.4 \text{ MHz} \quad \text{for } J = 12.5. \tag{10b}$$

The electric quadrupole hfs of this molecule was discussed by Mizushima,[26] Lin and Mizushima,[27] and Gallagher and Johnson.[6] This effect may contribute up to 1 MHz to each hfs in the states of our present interest. Due to inaccuracies in the magnetic hfs calculation resulting from a long-range extrapolation, it was decided that a calculation of the electric quadrupole hfs was not warranted for our present purpose. The discussion of this effect will be postponed to a later paper.[23]

The magnetic g factor of this type of molecules has been discussed by Radford[28] and Mizushima.[1] MM[1] showed that the g factor of each state can be expressed as

$$g_{c2} = g_\xi(J) + g_\eta(J) + g_X(J) + g_Y(J), \tag{11a}$$

$$g_{d2} = g_\xi(J) - g_\eta(J) + g_X(J) - g_Y(J), \tag{11b}$$

$$g_{c1} = g_\xi(J) + g_\eta(J) - g_X(J) - g_Y(J), \tag{11c}$$

$$g_{d1} = g_\xi(J) - g_\eta(J) - g_X(J) + g_Y(J), \tag{11d}$$

where, if the spin g factor is assumed as exactly 2 and smaller terms are all neglected,

$$g_\xi(J) = \frac{3}{2J(J+1)} + g_n , \tag{12a}$$

$$g_\eta(J) = -\frac{\psi(J+\frac{1}{2})}{4J(J+1)} , \tag{12b}$$

$$g_X(J)=\{3\bar{A}_J-4\bar{B}_J[(J+\tfrac{1}{2})^2-1]\}/[2X_JJ(J+1)], \tag{12c}$$

$$g_Y(J)=\frac{\bar{A}_J\psi(J+\frac{1}{2})}{4X_JJ(J+1)}\ , \tag{12d}$$

where ψ is a coupling constant defined by MM.[1] According to Mizushima, Cox, and Gordy[15] $\psi=0.0037$ for this molecule. We do not know much about the value of g_n, the contribution due to the end-over-end rotation, except that it is about 0.001 in magnitude. In any case we obtain

$$\begin{aligned} &g_\ell=0.0104+g_n,\quad g_X=-0.016\,76 \text{ for } J=11.5,\\ &g_\ell=0.0089+g_n,\quad g_X=-0.018\,08 \text{ for } J=12.5,\\ &g_n\cong -g_Y\cong -0.000\,075 \qquad \text{for both cases.}\end{aligned} \tag{13}$$

The second-order effects are not negligible. Complicated formulas shown in the Appendix give

$$\alpha f_2=(\mu_B\mathcal{H})^2\left\{\left(\frac{\bar{A}}{X_J}\right)^4\left[\frac{M^2}{X_JJ^2}+\frac{2X_J(J^2-M^2)}{X_J^2-4(BJ)^2}\left(\frac{2B}{\bar{A}}+\frac{1}{4J}\right)^2\right]+\frac{\bar{A}}{8X_J^2}\left(1+\frac{4\bar{A}}{BJ^2}\right)\left(1-\frac{3M^2}{J^2}\right)\right\}, \tag{14a}$$

$$\alpha f_1=-(\mu_B\mathcal{H})^2\left\{\left(\frac{\bar{A}}{X_J}\right)^4\left[\frac{M^2}{X_JJ^2}+\frac{2X_J(J^2-M^2)}{X_J^2-4(BJ)^2}\left(\frac{2B}{A}+\frac{1}{4J}\right)^2\right]-\frac{\bar{A}}{8X_J^2}\left(1-\frac{3M^2}{J^2}\right)\right\}, \tag{14b}$$

as good approximations for the second-order effects when J is large enough. In these formulas $\mathcal{H}$ is the external magnetic field and μ_B is the Bohr magneton which is 1.3995 MHz/G (1 gauss $=10^{-4}T$). For $J=11.5$ and 12.5 they give (when $\mathcal{H}$ is in kG)

$$\left.\begin{aligned}\alpha f_2&=(0.496-0.003\,49M^2)\,\mathcal{H}^2 \quad \text{MHz}\\ \alpha f_1&=-(0.244+0.002\,23M^2)\,\mathcal{H}^2 \quad \text{MHz}\end{aligned}\right\}\ \text{for } J=11.5, \tag{15a}$$

$$\left.\begin{aligned}\alpha f_2&=(0.522-0.002\,94M^2)\,\mathcal{H}^2 \quad \text{MHz}\\ \alpha f_1&=-(0.294+0.001\,43M^2)\,\mathcal{H}^2 \quad \text{MHz}\end{aligned}\right\}\ \text{for } J=12.5. \tag{15b}$$

III. MAGNETIC AND ELECTRIC DIPOLE TRANSITIONS

Since the NO molecule has both electric and magnetic dipole moments, both electric and magnetic dipole transitions are possible. The electric dipole transition has a very small probability in this case, because it is forbidden in the $^2\Pi_{1/2}\rightarrow{}^2\Pi_{3/2}$ transition; the transition is possible only through a small fractional part of each wave function which gives the mixing of $^2\Pi_{1/2}$ into $^2\Pi_{3/2}$ and vice versa. In addition, the magnitude of the electric dipole moment is[29,30] only 0.158 Debye. Thus, it turns out that most of the transitions we observe here are magnetic dipole transitions, but we also observe some weak electric dipole transitions.

The probability[31,32] of the magnetic dipole transition for the $(^2\Pi_{1/2}{}^c_a JM)\rightarrow(^2\Pi_{3/2}{}^c_d JM)$ is

$$P^{(\mathrm{mg})}=\frac{32\nu\omega^3}{3\pi\hbar\epsilon_0(2c)^5}\,\mu_B^2\,\frac{[(J+\frac{1}{2})^2-1]M^2}{J^2(J+1)^2}\,\delta(\omega-\omega_0), \tag{16a}$$

where ν and ω are the photon number and photon frequency while ω_0 is the molecular frequency of the transition. The corresponding probability of the electric dipole transition for the $(^2\Pi_{1/2}{}^c_d JM)\rightarrow(^2\Pi_{3/2}{}^d_c JM)$ is (here the designations $^2\Pi_{1/2}$ and $^2\Pi_{3/2}$ are only approximate)

$$P^{(\mathrm{el})}=\frac{32\nu\omega^3}{3\pi\hbar\epsilon_0(2c)^3}\,\frac{(AB)^2}{X_J^4}\,\frac{[(J+\frac{1}{2})^2-1]M^2}{J^2(J+1)^2}\,\delta(\omega-\omega_0), \tag{16b}$$

where μ is the electric dipole moment. When we take the known numbers for A, B, μ, and μ_B, and take $X_J=127\ \mathrm{cm}^{-1}$, we obtain

$$P^{(\mathrm{mg})}/P^{(\mathrm{el})}=21 \tag{17}$$

as the ratio of the intensities of these transitions.

Since we use linearly polarized laser light we see that when the magnetic transition is such that $\Delta M=0$ the electric transition obeys the selection rule $\Delta M=\pm1$, and vice versa. For $(J,M)\rightarrow(J,M\pm1)$ transitions, one should replace M^2 in (16a) and/or (16b) by $\frac{1}{4}[J(J+1)-M(M\pm1)]$. In the case of $J\rightarrow J-1$, the M dependence of the transition probabilities is known to be J^2-M^2 for $\Delta M=0$ and $\frac{1}{4}[(J\mp M)(J\mp M-1)]$ for $\Delta M=\pm1$ transitions. These relations are observed in the 119-μm resonances.

IV. EXPERIMENT

The laser-magnetic-resonance spectrometer is shown in Fig. 3. The laser oscillates between mirrors C and D and is divided into two parts by the dielectric beam splitter. The sample is in one part and the active medium of the laser is in the other. The beam splitter restricts the field of the laser to linear polarization. A valve (not shown) permits the connection of both sides for simultaneous evacuation in order to protect the beam splitter. The beam splitter can be rotated from the Brewster angle to increase the coupling to the laser cavity. Detector A was used to set the laser to the center of the laser line, and detector B fed the amplifier synchronized with the modulation coil modulated at 84 Hz. A 15-in. magnet with $5\frac{1}{2}$-in. Rose shimmed

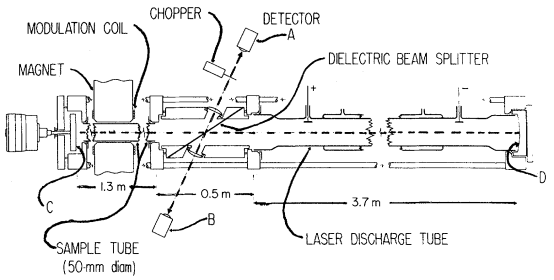

FIG. 3. Schematic diagram of the apparatus.

pole tips was used; it permitted fields up to 23.5 kG. Modulation amplitudes of 5, 10, or 16 G were used depending on the linewidths of the NO resonances.

The magnetic field strength at the center of certain lines were accurately measured with an NMR gaussmeter and frequency counter. A correction was made for the difference in field strength between the NMR location and the center of the sample cell.

Standard golay cells were used as detectors at 84 Hz. Detector B received the full laser output of a few milliwatts; no saturation of this detector was observed apparently because the signal was a small ac signal superposed on the large dc-laser-output signal. Figure 4 shows the experimental result.

V. EXPERIMENTAL RESULTS AND THEIR INTERPRETATION

A. 78-μm Parallel Resonances

As explained before, the 78-μm resonances are due to the transitions $(^2\Pi_{1/2}J=12.5)\rightarrow(^2\Pi_{3/2}J=12.5)$. When the magnetic component of the laser field is parallel to the external magnetic field, the magnetic dipole transitions obey the selection rule $\Delta M=0$ and the intensity is proportional to M^2.

Two sets of resonances are observed. The first set which starts at about 1.419 kG is due to the $c1\rightarrow c2$ (that is, $^2\Pi_{1/2}\rightarrow{}^2\Pi_{3/2}c$) transitions, and the second set which starts at 7.883 kG is due to the $d1\rightarrow d2$ transitions. The first set has a complicated structure due to the overlapping and other interactions between hfs components, while in the second set the hfs is completely decoupled and simply makes each component a triplet.

The magnetic field of the central component ($M_I=0$ component) of each triplet is measured carefully for the second set. The resultant values are given in Table I with their assignment. Lines listed in the various tables are indicated in Fig. 4. These resonance fields are reproduced by

$$M\mathcal{B}=97.8\mathcal{B}+0.0163\mathcal{B}^2(1-0.00185M^2). \quad (18)$$

It is easy to obtain

$$(g_{d1}-g_{d2})\mu_B M\mathcal{B}=f_{d2}-f_{d1}-\hbar\omega_0+(\Delta f_{d2}-\Delta f_{d1}), \quad (19)$$

where f_{d2} and f_{d1} are the energies of the $d2$ and $d2$ states when $\mathcal{B}=0$, ω_0 is the laser frequency which is reported[21] as 3.821775 THz, and Δf_{d2} and Δf_{d1} are the second-order effects we calculated in (15b). Comparing (18) with (19) we obtain

$$f_{d2}(12.5)-f_{d1}(12.5)=0.1369(g_{d1}-g_{d2})+3.821775\ \text{THz}. \quad (20)$$

Each line of the second set is a triplet with separation of 67 ± 2 G. The corresponding hfs coupling constant is

$$|a_{d2}-a_{d1}|=15.7(g_{d1}-g_{d2})\ \text{GHz}. \quad (21)$$

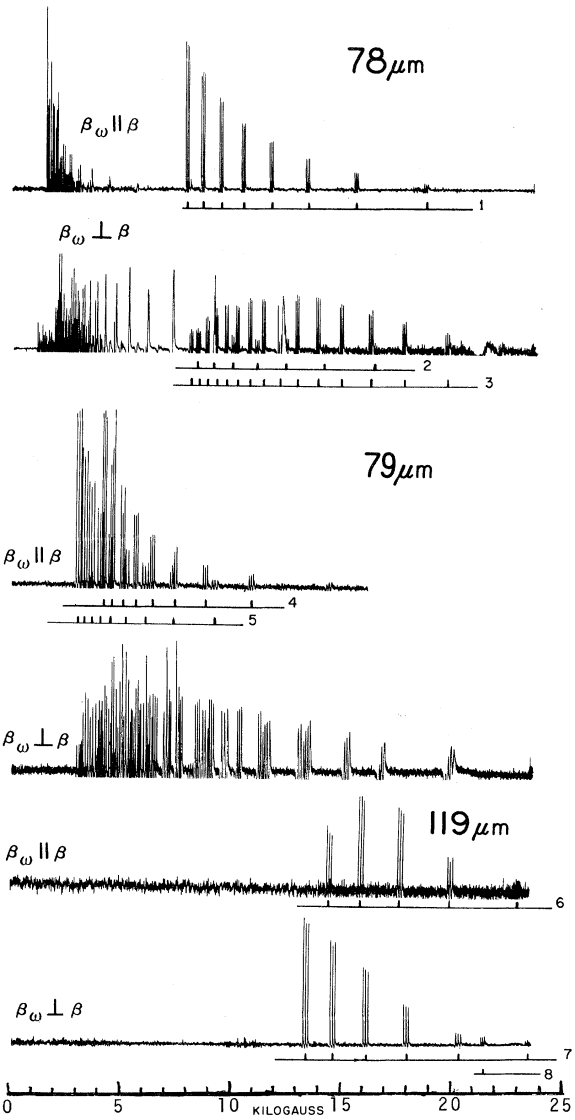

FIG. 4. Typical chart recorder traces of the laser magnetic resonances of the NO molecule. The lower-half of each trace is cut out to save space. The numbers 1–8 refer to tables where magnetic fields for the indicated lines are tabulated.

TABLE I. Resonance magnetic fields in kilogauss for $(d1\ 12.5\ M) \rightarrow (d2\ 12.5\ M)$ magnetic transitions ($M_I = 0$ components).

$\mathcal{B}$ [a]	7.882	8.584	9.434	10.453	11.74	13.40	15.63	18.82
M	12.5	11.5	10.5	9.5	8.5	7.5	6.5	5.5
$\mathcal{B}_{calc}$	7.882	8.584	9.426	10.452	11.74	13.39	15.62	18.80

[a]Uncertainty is ±1 in the last digits.

The first set is too complicated to allow a similar analysis, but we can see that

$$M\mathcal{B} = 18.75 \pm 0.15, \tag{22}$$

which implies that

$$f_{c2}(12.5) - f_{c1}(12.5) = 0.0260(g_{c1} - g_{c2}) + 3.821775\ \text{THz}. \tag{23}$$

B. 78-μm Perpendicular Resonances

In this polarization both magnetic dipole and electric dipole transitions are observed. Since the selection rules are different, namely, $(c\,M) \rightarrow (c\,M \pm 1)$ and $(d\,M) \rightarrow (d\,M \pm 1)$ for the magnetic dipole and $(c\,M) \rightarrow (d\,M)$ and $(d\,M) \rightarrow (c\,M)$ for the electric dipole transitions, these two types of resonances occur at different field strength.

Again there are two sets; those resonances below 8 kG are due to $c1 \rightarrow c2$ or $c1 \rightarrow d2$, and those above 8 kG are due to the $d1 \rightarrow d2$ or $d1 \rightarrow c2$ transitions.

The first set is quite complicated, but is clearly made of two series; a weak one which starts at 0.93 kG and a strong one which starts at about 1.73 kG. The former is interpreted as the electric dipole transitions $(c1\,M) \rightarrow (d2\,M)$, and the latter is interpreted as the magnetic dipole transitions $(c1\,M) \rightarrow (c2\ M \pm 1)$. From the weaker series we obtain

$$f_{d2}(12.5) - f_{c1}(12.5) = 0.0166(g_{c1} - g_{d2}) + 3.821775\ \text{THz}. \tag{24}$$

In the second set each resonance is a well-defined triplet, except that the superposition of the electric series and magnetic series makes the appearance more complicated. The $M_I = 0$ components of the electric transitions are given in Table II with their assignment. These resonance fields can be reproduced by

$$M\mathcal{B} = 103.9 + 0.016\mathcal{B}^2(1 - 0.019M^2). \tag{25}$$

The values of $\mathcal{B}$ calculated from this equation are also given in Table II. In the same way as we interpreted (18) we obtain

$$f_{c2}(12.5) - f_{d1}(12.5)$$

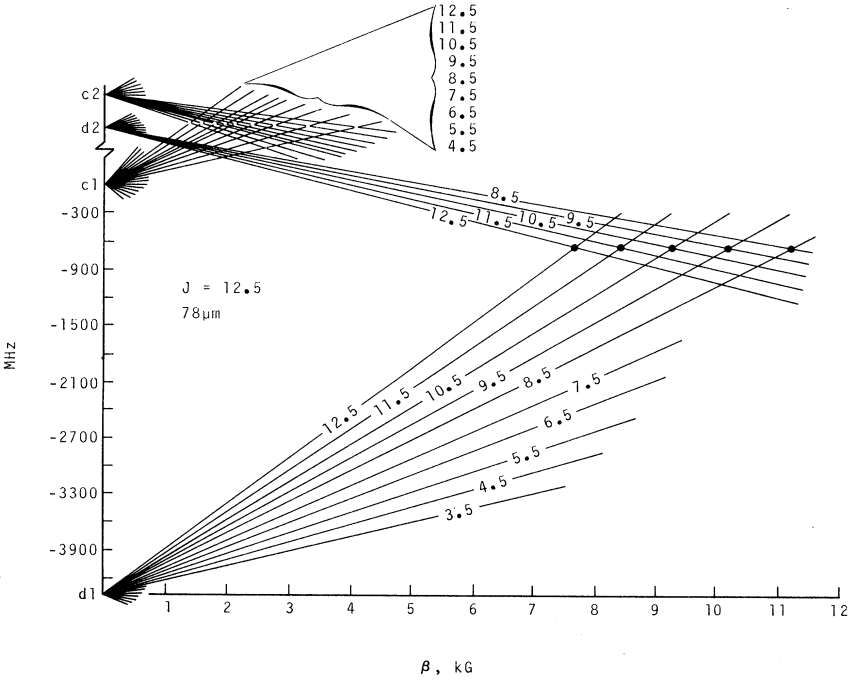

FIG. 5. Energy levels of the $J = 12.5$ states. The $(c2)$ and $(d2)$ levels are shifted down by the frequency of the 78-μm laser line. Therefore, appropriate levels of $(c1\,M'')$ and $(c2\,M')$, for example, cross each other at the resonance field for that magnetic transition. Only $\Delta M = 0$ magnetic transitions are indicated by dots.

TABLE II. Resonance magnetic fields in kilogauss for $(d1\ 12.5\ M) \rightarrow (c2\ 12.5\ M)$ electric transitions ($M = 0$ components).

$\mathcal{B}$ [a]	8.34	9.07	9.98	11.07	12.43	14.19
M	12.5	11.5	10.5	9.5	8.5	7.5
$\mathcal{B}_{calc}$	8.34	9.07	9.95	11.02	12.35	14.06

[a]Uncertainty is ±15 G.

$$= 0.1456(g_{d1} - g_{c2}) + 3.821775 \text{ THz}. \quad (26)$$

The triplet separation in this series is 68 ± 2 G, which gives

$$|\mathcal{B}_{c2} - \mathcal{B}_{d1}| = 16.1(g_{d1} - g_{c2}) \text{ GHz}. \quad (27)$$

The stronger series in the second set is due to the magnetic dipole transitions $(d1\,M) \rightarrow (d2\,M \pm 1)$, and the resonance fields are given in Table III, which also gives their assignment and the values calculated by

$$M\mathcal{B} = 97.494 + 0.0163\,\mathcal{B} \pm 0.25\,\mathcal{B}, \quad (28)$$

where the double sign means plus for $M \rightarrow M+1$ and minus for $M \rightarrow M-1$ transitions, and M is the average M value of the transition; namely, if the transition is $M'' \rightarrow M'$, then

$$M = \tfrac{1}{2}(M'' + M'). \quad (29)$$

Corresponding to (19) we obtain

$$(g_{d1} - g_{d2})M\mu_B\mathcal{B} = f_{d2} - f_{d1} - \hbar\omega_0 + (a_2 + b_2 - a_1 - b_1)\mathcal{B}^2 - (b_2 - b_1)M^2\mathcal{B}^2 \pm [\tfrac{1}{2}(g_{d2} + g_{d1})\mu_B - (b_2 - b_1)M\mathcal{B}]\mathcal{B}, \quad (30)$$

if M is defined by (29), and

$$\mathcal{B} f_{d2} = (a_2 + b_2 M_{d2}^2)\mathcal{B}^2, \quad (31a)$$

$$\mathcal{B} f_{d1} = (a_1 + b_1 M_{d1}^2)\mathcal{B}^2. \quad (31b)$$

Comparing (28) with (30) we obtain

$$g_{d1} + g_{d2} = 0.50(g_{d1} - g_{d2}). \quad (32)$$

The triplet separation in this series agrees with Eq. (21). Equation (21) is found to be applicable to this series also.

C. 79 - μm Parallel Resonances

The resonances at 79 μm are because of the transitions similar to those at 78 μm except that $J = 11.5$, instead of 12.5. Here the spectrum looks more complicated because the laser frequency is so close to $X_{11.5}$ that two sets of resonances due to $(c1\,M) \rightarrow (c2\,M)$ and $(d1\,M) \rightarrow (d2\,M)$, respectively, overlap each other. Tables IV and V list these two sets separately. Each line is made of a well-defined triplet due to the hfs.

TABLE III. Resonance magnetic fields in kilogauss for $(d1\ 12.5\ M_{d1}) \rightarrow (d2\ 12.5\ M_{d2})$ magnetic transitions ($M_I = 0$ components).

$\mathcal{B}$ [a]	8.05	8.395	8.775	9.20	9.665	10.17	10.75	11.38	12.12	12.92	13.88	14.97	16.30	17.87	19.86
M_{d2}	11.5	12.5	10.5	11.5	9.5	10.5	8.5	9.5	7.5	8.5	6.5	7.5	5.5	6.5	4.5
M_{d1}	12.5	11.5	11.5	10.5	10.5	9.5	9.5	8.5	8.5	7.5	7.5	6.5	6.5	5.5	5.5
$\mathcal{B}_{calc}$	8.05	8.395	8.87	9.20	9.66	10.18	10.75	11.39	12.11	12.93	13.89	14.92	16.30	17.86	19.80

[a]Uncertainty is ±15 G.

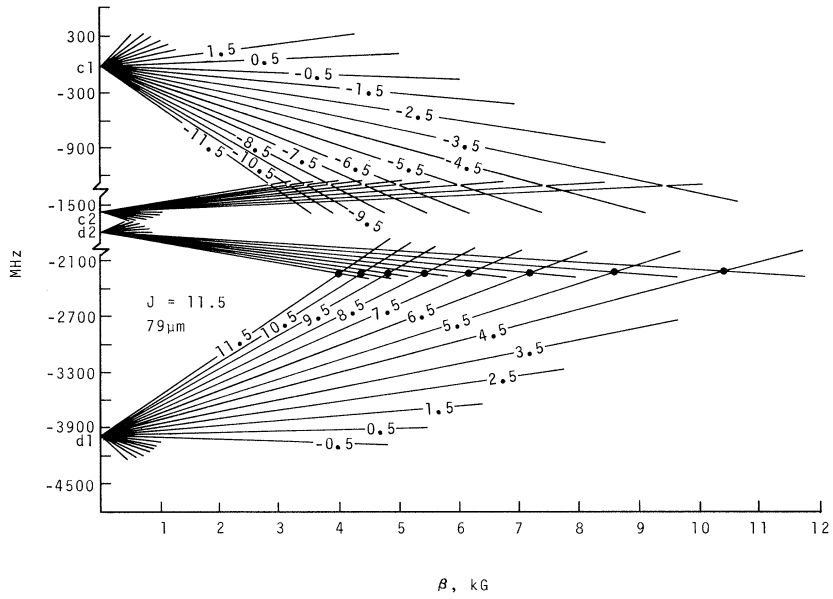

FIG. 6. Energy levels of the $J=11.5$ states. The ($c2$) and ($d2$) levels are shifted down by the frequency of the 79-μm laser line. Only $\Delta M=0$ magnetic transitions are indicated by dots.

The $M_I=0$ components of $(c1M)\rightarrow(c2M)$ resonances are fit by

$$M\mathcal{B}=33.497+0.01731\mathcal{B}^2(1-0.00170M^2). \quad (33)$$

while those of the $(d1M)\rightarrow(d2M)$ resonances are fit by

$$M\mathcal{B}=46.6391+0.0173\mathcal{B}^2(1-0.00170M^2), \quad (34)$$

Calculated values of the resonance fields are also shown in Tables IV and V. These formulas give (using the recently measured frequency[20] of this laser line)

$$f_{c2}-f_{c1}=-0.04628(g_{c1}-g_{c2})+3.790477\ \text{THz} \quad (35)$$

and

$$f_{d2}-f_{d1}=0.06527(g_{d1}-g_{d2})+3.790477\ \text{THz} \quad (36)$$

The signs of the first terms in the above formulas are determined theoretically from the corresponding signs of the second-order-effect terms in (33) and (34).

The hfs of the $(c1M=11.5)\rightarrow(c2M=11.5)$ line is measured carefully. From the splitting of 112.43 G we obtain

$$|\mathcal{A}_{c2}-\mathcal{A}_{c1}|=22.618(g_{c1}-g_{c2})\ \text{GHz}. \quad (37)$$

The splitting in the other transitions $(d1M)\rightarrow(d2M)$ is observed to be 83 G, which gives

$$|\mathcal{A}_{d2}-\mathcal{A}_{d1}|=16.8(g_{d1}-g_{d2})\ \text{GHz}. \quad (38)$$

A large number of resonance lines are observed in the 79-μm perpendicular case, but the spectrum is so complicated that we did not attempt to measure these resonance fields carefully nor analyze them.

D. 119-μm Parallel Resonances

Four resonances, each of which is a triplet, are observed. Table VI shows the observed $M_I=0$ components and the values calculated by

$$M\mathcal{B}=163.5+0.019\mathcal{B}^2(1-0.0026M^2). \quad (39)$$

This formula gives

$$f_{d2}(11.5)-f_{c1}(12.5)=0.2290[g_{c1}(12.5)-g_{d2}(11.5)]+2.527953\ \text{THz} \quad (40)$$

when they are interpreted as the $(c1J=12.5M)\rightarrow(d2J=11.5M)$ magnetic dipole transitions.

The hfs splitting is 111.001 G, which gives

$$\left|\frac{\mathcal{A}_{d2}(11.5)}{11.5}-\frac{\mathcal{A}_{c1}(12.5)}{13.5}\right|$$

TABLE IV. Resonance magnetic fields in kilogauss for ($c1$ 11.5 M) $\rightarrow$ ($c2$ 11.5 M) magnetic transitions ($M_I=0$ components).

$\mathcal{B}$ [a]	2.9037	3.175	3.5067	3.915	4.425	5.092	5.980	7.235	9.15
M	−11.5	−10.5	−9.5	−8.5	−7.5	−6.5	−5.5	−4.5	−3.5
$\mathcal{B}$ calc	2.9030	3.177	3.5070	3.913	4.426	5.089	5.984	7.25	9.17

[a]Uncertainty is about ±3 in the last digits.

TABLE V. Resonance magnetic fields in kilogauss ($d1\ 11.5\ M$) → ($d2\ 11.5\ M$) magnetic transitions ($M_I = 0$ components).

ℬ [a]	4.075	4.4686	4.96	5.5421	6.3019	7.309	8.705	10.805
M	11.5	10.5	9.5	8.5	7.5	6.5	5.5	4.5
$ℬ_{calc}$	4.075	4.4687	4.95	5.5420	6.3017	7.308	8.707	10.80

[a]Uncertainty is about ±3 in the last digits.

$$= 1.9418[g_{c1}(12.5) - g_{d2}(11.5)]\ \text{GHz}. \quad (41)$$

E. 119 - μm Perpendicular Resonances

All observed resonances, which are listed in Table VII, are the ($c1\,J = 12.5\,M$) → ($d2\,J = 11.5\,M - 1$) transitions. The other series $M \rightarrow M+1$ is expected to be of much lower intensity and was not observed. Table VII also gives calculated values from

$$M ℬ = 162.2 + 0.019\,ℬ^2 \pm 0.311 ℬ\ , \quad (42)$$

where M is defined by (29) and only the lower sign of the double sign is used in Table VII. Comparing this result with a formula similar to (30) we obtain

$$g_{c1}(12.5) + g_{d2}(11.5) = 0.622[g_{c1}(12.5) - g_{d2}(11.5)]. \quad (43)$$

The hfs splitting of this series is the same as (41).

One triplet at 21.55, 21.63, and 21.72 kG does not fit in the series given by (42), and is interpreted as the ($d1\,J = 12.5\,M = 12.5$) → ($c2\,J = 11.5\,M = 11.5$) transition, where $ℬ = 21.63$, $M = 12.5$. There must be a corresponding resonance at about 22.5 kG in the parallel case due to ($d1\,J = 12.5\,M = 11.5$) → ($c2\,J = 11.5\,M = 11.5$) if this interpretation is correct. The resonance, however, was not found, probably because the intensity is low [the intensity of (JM) → ($J - 1\,M$) transition is proportional to $J^2 - M^2$] and because the experimental sensitivity is decreased due to increasing magnetic field inhomogeneity at high fields. With this interpretation we obtain

$$M ℬ = 262.9 + 0.019\,ℬ^2(1 - 0.0026M^2), \quad (44)$$

where the second-order-effect terms are assumed to be the same as (39). From (44) we obtain

$$f_{c2}(11.5) - f_{d1}(12.5) = 0.3679[g_{d1}(12.5) - g_{c2}(11.5)]$$
$$+ 2.527\,953\ \text{THz}. \quad (45)$$

From the hfs splitting of this triplet we obtain

$$\left| \frac{a_{c2}(11.5)}{11.5} - \frac{a_{d1}(12.5)}{13.5} \right| = 1.49[g_{d1}(12.5) - g_{c2}(11.5)]\ \text{GHz}. \quad (46)$$

VI. g FACTORS AND ENERGY LEVELS

The g factors are given in (11) and (12), and their values for $J = 11.5$ and 12.5 are estimated in (13). Since g_η and g_Y are expected to be very small we can assume that

$$g_{c2} - g_{c1} \cong g_{c2} - g_{d1} \cong g_{d2} - g_{c1} \cong g_{d2} - g_{d1} \cong 2g_X \quad (47)$$

hold within the accuracy of 1%.

The energy differences in the $J = 12.5$ states are given by (20), (23), (24), and (26) in terms of the g factors. We notice that (20) + (23) = (24) + (26) should hold among these equations, and we actually see that this relation holds within the accuracy of about 0.5%, which indicates the experimental accuracy of energy levels that we are going to evaluate now. We cannot reduce this inaccuracy even when g_η and g_Y are included.

In Sec. II we have estimated the values of the g factors and the energy levels. We have reasons to believe that the estimated values of g_X have better accuracy than those of the energy levels. Therefore, we assume that (13) is correct and evaluate the energy levels from our experimental data. Thus, from (20), (23), (24), and (26), we obtain

$$f_{c2}(12.5) - f_{d2}(12.5) = 2\eta_{12.5} + (Y_{12.5}/2X_{12.5}) = -(0.0170 \pm 0.0003)g_X\ \text{THz} = 307 \pm 5\ \text{MHz}, \quad (48)$$

TABLE VI. Resonance magnetic fields in kilogauss for ($c1\ J = 12.5\ M$) → ($d2\ J = 11.5\ M$) magnetic transitions. ($M_I = 0$ components).

ℬ	14.44	15.895	17.69	19.975	23.05
M	11.5	10.5	9.5	8.5	7.5
$ℬ_{calc}$	14.44	15.90	17.70	19.98	22.98

TABLE VII. Resonance magnetic fields in kilogauss for ($c1\ J = 12.5\ M$) → ($d2\ J = 11.5\ M - 1$) magnetic transitions ($M_I = 0$ components).

ℬ	13.464	14.713	16.226	18.099	20.51	23.74
M	12.5	11.5	10.5	9.5	8.5	7.5
$ℬ_{calc}$	13.463	14.712	16.226	18.099	20.49	23.65

$$f_{c1}(12.5)-f_{d1}(12.5)=2\eta_{12.5}-(Y_{12.5}/2X_{12.5})$$
$$=-(0.2400\pm 0.0003)g_X \text{ THz}$$
$$=4340\pm 20 \text{ MHz}, \quad (49)$$

$$X_{12.5}=-(0.1624\pm 0.0003)g_X+3.821\,775 \text{ THz}$$
$$=3.824\,711 \text{ THz}\pm 15 \text{ MHz}$$
$$=127.5786\pm 0.0005 \text{ cm}^{-1}, \quad (50)$$

for the $J=12.5$ states. We see that (48) and (49) agree well with our predictions (5c) and (5d). The value of $X_{12.5}$ obtained here is slightly different from the predicted value in (4) indicating that A must be slightly less than the previously accepted value of Keck and Hause.[10]

From the 79-μm resonances we obtain

$$f_{c2}(11.5)-f_{c1}(11.5)=3.790\,477-0.001\,566 \text{ THz} \quad (51)$$

and

$$f_{d2}(11.5)-f_{d1}(11.5)=3.790\,477+0.002\,180 \text{ THz} \quad (52)$$

from (13), (35), and (36). Therefore, we find

$$X_{11.5}=3.790\,784 \text{ THz}\pm 15 \text{ MHz}$$
$$=126.4469\pm 0.0005 \text{ cm}^{-1}. \quad (53)$$

This value of $X_{11.5}$ is again smaller than the predicted one given in (4).

From (52) and (53) we obtain

$$f_{c2}(11.5)-f_{d2}(11.5)-[f_{c1}(11.5)-f_{d1}(11.5)]$$
$$=-3746\pm 20 \text{ MHz}, \quad (54)$$

which is in fair agreement with the predicted values (5a) and (5b).

From the 119-μm resonances we obtain

$$f_{d2}(11.5)-f_{c1}(12.5)=2.527\,9540+0.007\,65 \text{ THz} \quad (55)$$

and

$$f_{2c}(11.5)-f_{d1}(12.5)=2.527\,9540+0.012\,29 \text{ THz}. \quad (56)$$

The difference

$$f_{c1}(12.5)-f_{d1}(12.5)+f_{c2}(11.5)-f_{d2}(11.5)=4638 \text{ MHz} \quad (57)$$

is to be compared with the predicted value 4566 MHz given by (5a) and (5d).

The hfs coupling constants obtained by assuming the g factors of (13) are

$$|a_{d2}(12.5)-a_{d1}(12.5)|=568 \text{ MHz}, \quad (58a)$$
$$|a_{c2}(12.5)-a_{d1}(12.5)|=583 \text{ MHz}, \quad (58b)$$
$$|a_{c2}(11.5)-a_{c1}(11.5)|=758 \text{ MHz}, \quad (58c)$$
$$|a_{d2}(11.5)-a_{d1}(11.5)|=563 \text{ MHz}, \quad (58d)$$
$$\left|\frac{a_{d2}(11.5)}{11.5}-\frac{a_{d1}(12.5)}{13.5}\right|=64.9 \text{ MHz}, \quad (58e)$$
$$\left|\frac{a_{c2}(11.5)}{11.5}-\frac{a_{d1}(12.5)}{13.5}\right|=49.8 \text{ MHz}, \quad (58f)$$

which are obtained from (21), (27), (37), (41), and (46), respectively. These values agree with the predicted values obtained from (10a) and (10b) within 15%, which is within the accuracy of the predicted values.

The two relations (32) and (43) between the g factors are obeyed by the values given in (13) within 0.5%, when g_n is neglected.

The second-order-effect terms given in (18), (25), (33), (34), (39), (40), and (42) all agree with the theoretical values given in (15a) and (15b) within 10%. In these formulas the coefficients of the $M^2\mathcal{R}^2$ terms are taken in such a way that their ratios to the corresponding $\mathcal{R}^2$ terms agree with theory.

VII. SPIN-ORBIT COUPLING CONSTANT

If we assume that

$$\bar{B}_{11.5}=\bar{B}_{12.5}=\langle B\rangle\approx B-\tfrac{1}{2}\mu_s-\tfrac{1}{2}\alpha-300D \quad (59)$$

and

$$\bar{A}_{11.5}=\bar{A}_{12.5}=\langle A\rangle=A-2B+\beta+\tfrac{1}{4}\gamma-300(\delta-2D), \quad (60)$$

then we can obtain the values of $\langle B\rangle$ and $\langle A\rangle$ from (2c), (50), and (53). Thus,

$$\langle B\rangle=1.6955\pm 0.001 \text{ cm}^{-1} \quad (61)$$

and

$$\langle A\rangle=119.7682\pm 0.001 \text{ cm}^{-1}. \quad (62)$$

If we take the accepted values, $B=1.695\,79 \text{ cm}^{-1}$ and $D=5.5\times 10^{-6} \text{ cm}^{-1}$, we see that

$$B-2D(J+\tfrac{1}{2})^2=1.6942 \text{ cm}^{-1} \text{ for } J=11.5 \text{ and } 12.5, \quad (63)$$

which is in fair agreement with (61). On the other hand we know that $\alpha\cong 0.006 \text{ cm}^{-1}$. Therefore, from (3b) we obtain

$$\mu_S(\cong-\alpha)=-0.006\pm 0.002 \text{ cm}^{-1}. \quad (64)$$

This value might be compared with 0.008 cm^{-1} for the O_2 molecule.[31]

From (3a) we obtain

$$A-300\delta+\tfrac{1}{4}\gamma=\langle A\rangle+2B-600D-\beta$$
$$=123.1580\pm 0.001 \text{ cm}^{-1}. \quad (65)$$

The value of γ cannot be obtained from experiment, but may be estimated[1] as

$$\gamma\cong\alpha^2/\beta=0.90 \text{ cm}^{-1}. \quad (66)$$

Thus, we find

$$A - 300\delta = 122.93\ \text{cm}^{-1}. \tag{67}$$

In order to know A itself we have to find δ by measuring X_J in other rotational states with high accuracy.

In less-accurate conventional theories the quantity given in (65) is called the spin-orbit coupling constant. We see that the value given in (65) agrees with the older value obtained by James and Thibault[9] and Hall and Dowling,[4] and is somewhat smaller than the more recent value proposed by Keck and Hause.[10] In any case, since the transition frequencies we observed are the most sensitive to the value of the coupling constant, we believe the value given in (65) is more accurate than any previously reported values.

ACKNOWLEDGMENT

We thank Professor A. Dymanus for showing us his unpublished data.

APPENDIX: SECOND-ORDER EFFECTS

When we define

$$\hat{\mathcal{H}} = \mu_B \vec{\mathcal{B}} \cdot (2\vec{S} + \vec{L}) \tag{A1}$$

we obtain

$$\langle {}^c_d 2JM \mid \hat{\mathcal{H}} \mid {}^c_d 1JM \rangle = \frac{M\{-\bar{A}^2 - 6\bar{A}B + 4B^2[(J+\tfrac{1}{2})^2 - 1]\}[(J+\tfrac{1}{2})^2 - 1]^{1/2}}{X_J^2\, J(J+1)}\, \mu_B \mathcal{B}, \tag{A2}$$

$$\langle {}^c_d 2JM \mid \hat{\mathcal{H}} \mid {}^d_c 1J+1M \rangle = [(J+1)^2 - M^2]^{1/2} \Big\{ -\tfrac{1}{2}\bar{A}^2[(J+1)^2 - 2(J+1) + 0.75]^{1/2} - 4\bar{A}B\{[(J+1.5)^2 - 1][(J+1)^2 - 2.25]\}^{1/2}$$
$$+ 2B^2\{[(J+\tfrac{1}{2})^2 - 1][(J+1.5)^2 - 1][(J+1)^2 + 2(J+1) + 0.75]\}^{1/2} \Big\}$$
$$\times \{X_J X_{J+1}(J+1)[4(J+1)^2 - 1]^{1/2}\}^{-1} \mu_B \mathcal{B}, \tag{A3}$$

$$\langle {}^c_d 2JM \mid \hat{\mathcal{H}} \mid {}^d_c 1J-1M \rangle = (J^2 - M^2)^{1/2} \Big\{ -\tfrac{1}{2}\bar{A}^2(J^2 + 2J + 0.75)^{1/2} - 4\bar{A}B\{[(J-\tfrac{1}{2})^2 - 1](J^2 - 2.25)\}^{1/2}$$
$$+ 2B^2\{[(J+\tfrac{1}{2})^2 - 1][(J-\tfrac{1}{2})^2 - 1](J^2 - 2J + 0.75)\}^{1/2}] \Big\} \ [X_{J-1} X_J J(4J^2 - 1)^{1/2}]^{-1} \mu_B \mathcal{B}, \tag{A4}$$

$$\langle {}^c_d 2JM \mid \mathcal{H} \mid {}^d_c 2J-1M \rangle = (J^2 - M^2)^{1/2} \Big\{ 2\bar{A}^2(J^2 - 2.25)^{1/2} - \bar{A}B\{[(J+\tfrac{1}{2})^2 - 1]^{1/2}(J^2 - 2J + 0.75)^{1/2}$$
$$+ [(J-\tfrac{1}{2})^2 - 1]^{1/2}(J^2 + 2J + 0.75)^{1/2}\} \Big\} [X_J X_{J-1} J(4J^2 - 1)^{1/2}]^{-1} \mu_B \mathcal{B}, \tag{A5}$$

$$\langle {}^c_d 2JM \mid \mathcal{H} \mid {}^d_c 2J+1M \rangle$$
$$= [(J+1)^2 - M^2]^{1/2} \Big\{ 2\bar{A}^2[(J+1)^2 - 2.25]^{1/2} - \bar{A}B\{[(J+\tfrac{1}{2})^2 - 1]^{1/2}[(J+1)^2 + 2(J+1) + 0.75]^{1/2}$$
$$+ [(J+1.5)^2 - 1]^{1/2}[(J+1)^2 - 2(J+1) + 0.75]^{1/2}] \Big\} \{X_{J+1} X_J (J+1)[4(J+1)^2 - 1]^{1/2}\}^{-1} \mu_B \mathcal{B}, \tag{A6}$$

$$\langle {}^c_d 1JM \mid \mathcal{H} \mid {}^d_c 1J-1M \rangle = \bar{A}B(J^2 - M^2)^{1/2} \{ [(J+\tfrac{1}{2})^2 - 1]^{1/2}(J^2 + 2J + 0.75)^{1/2}$$
$$+ [(J-\tfrac{1}{2})^2 - 1]^{1/2}(J^2 - 2J + 0.75)^{1/2}\} [X_J X_{J-1} J(4J^2 - 1)^{1/2}]^{-1} \mu_B \mathcal{B}, \tag{A7}$$

$$\langle {}^c_d 1JM \mid \mathcal{H} \mid {}^d_c 1J+1M \rangle$$
$$= \bar{A}B[(J+1)^2 - M^2]^{1/2} \Big\{ [(J+\tfrac{1}{2})^2 - 1]^{1/2}\{(J+1)^2 - 2(J+1) + 0.75\}^{1/2} + [(J+1.5)^2 - 1]^{1/2}$$
$$\times [(J+1)^2 + 2(J+1) + 0.75]^{1/2} \Big\} \{X_{J+1} X_J (J+1)[4(J+1)^2 - 1]^{1/2}\}^{-1} \mu_B \mathcal{B}. \tag{A8}$$

In these formulas we find

$$\bar{A} = A - 2B. \tag{A9}$$

Plugging these matrix elements in the standard second-order perturbation formula we obtain the second-order-effect terms. When J is large the result reduces to (14a) and (14b).

---

*Work partially supported by the National Science Foundation under Grant No. GP-27444.

[1]M. Mizushima, Phys. Rev. (to be published), hereafter referred to as MM.

[2]J. H. Van Vleck, Phys. Rev. 33, 467 (1929).

[3]Except for the very recent experiment by J. M. Brown, A. R. H. Cole, and F. R. Honey (unpublished).

[4]R. T. Hall and J. M. Dowling, J. Chem. 45, 1899 (1966).

[5]C. A. Burrus and W. Gordy, Phys. Rev. 92, 1437 (1953).

[6]J. J. Gallagher and C. M. Johnson, Phys. Rev. 103, 1727 (1956); also, J. J. Gallagher, F. D. Bedard, and C. M. Johnson, Phys. Rev. 93, 729 (1954).

[7]P. G. Favero, A. M. Mirri, and W. Gordy, Phys. Rev. 114, 1534 (1959).

[8]A. Dymanus (private communication).

[9]T. C. James and R. J. Thibault, J. Chem. Phys. 41, 2806 (1964).

[10]D. B. Keck and C. D. Hause, J. Mol. Spectry. 26, 163 (1968).

[11]K. M. Evenson, H. P. Broida, J. S. Wells, R. J. Mahler, and M. Mizushima, Phys. Rev. Letters 21, 1038 (1968).

[12]K. M. Evenson and M. Mizushima, Phys. Rev. (to be published).

[13]K. M. Evenson, J. S. Wells, and H. E. Radford, Phys. Rev. Letters 25, 199 (1970).

[14]K. M. Evenson, H. E. Radford, and M. M. Moran, Jr., Appl. Phys. Letters 18, 426 (1971).

[15]M. Mizushima, J. T. Cox, and W. Gordy, Phys. Rev. 98, 1034 (1955).

[16]R. Beringer and J. G. Castel, Jr., Phys. Rev. 78, 581 (1950).

[17]G. C. Dousmanis, T. M. Sanders, Jr., and C. H. Townes, Phys. Rev. 100, 1735 (1955).

[18]L. Veseth, J. Mol. Spectry. 38, 228 (1971).

[19]R. S. Mulliken and A. Christy, Phys. Rev. 35, 87 (1931).

[20]The wave number of the 79-μm line is reported by W. S. Benedict, M. A. Pollack, and W. J. Tomlinson, III, IEEE J. Quantum Electron. QE-5, 108 (1969). The frequency of this line is now measured as 3.790 477 THz ±3 MHz by K. M. Evenson and J. S. Wells (unpublished).

[21]The frequency of the 78-μm line is measured by K. M. Evenson, J. S. Wells, L. M. Matarrese, and L. B. Elwell, Appl. Phys. Letters, 16, 159 (1970). The reported frequency is 3.821 775 THz.

[22]The frequency of the 119-μm line is measured by L. Frankel, T. Sullivan, M. A. Pollack, and T. J. Bridges, Appl. Phys. Letters 11, 344 (1967); and by L. O. Hocker and A. Javan, Phys. Letters 26A, 255 (1968). The reported values are 2.527 9528 and 2.527 954 0 THz, respectively.

[23]A. Dymanus and M. Mizushima (unpublished).

[24]R. A. Frosch and H. M. Foley, Phys. Rev. 88, 1337 (1952).

[25]G. C. Dousmanis, Phys. Rev. 97, 967 (1955).

[26]M. Mizushima, Phys. Rev. 94, 569 (1954).

[27]C. C. Lin and M. Mizushima, Phys. Rev. 100, 1726 (1955).

[28]H. E. Radford, Phys. Rev. 122, 114 (1961); 126, 1035 (1962).

[29]C. A. Burrus and J. D. Graybeal, Phys. Rev. 109, 1553 (1958).

[30]M. Mizushima, Phys. Rev. 109, 1557 (1958).

[31]See, for example, M. Mizushima, *Quantum Mechanics of Atomic Spectra and Atomic Structure* (Benjamin, New York, 1970), Chap. 4.

[32]B. G. West and M. Mizushima, Phys. Rev. 143, 31 (1966).